UNCLASSIFIED

RM No. E7A17a

NACA

RESEARCH MEMORANDUM

for the

Air Materiel Command, Army Air Forces

PERFORMANCE OF COMPRESSOR OF XJ-41-V TURBOJET ENGINE

I - PRELIMINARY INVESTIGATION AT EQUIVALENT COMPRESSOR SPEED OF 8000 RPM

By Ambrose Ginsburg and John W. R. Creagh

Aircraft Engine Research Laboratory
Cleveland, Ohio

NATIONAL ADVISORY COMMITTEE
FOR AERONAUTICS

WASHINGTON

JANUARY 17, 1947

UNCLASSIFIED

NATIONAL ADVISORY COMMITTEE FOR AERONAUTICS

RESEARCH MEMORANDUM

for the

Air Materiel Command, Army Air Forces

PERFORMANCE OF COMPRESSOR OF XJ-41-V TURBOJET ENGINE

I - PRELIMINARY INVESTIGATION AT EQUIVALENT COMPRESSOR SPEED OF 8000 RPM

By Ambrose Ginsburg and John W. R. Creagh

INTRODUCTION

At the request of the Air Materiel Command, Army Air Forces, an investigation is being conducted at the NACA Cleveland laboratory to determine the performance characteristics of the XJ-41-V turbojet-engine compressor.

The complete compressor was mounted on a collecting chamber having an annular air-flow passage simulating the burner annulus of the engine and was driven by an electric motor. The compressor was extensively instrumented to determine the over-all performance of the compressor, the characteristic performance of each of the compressor components, the state of the air stream in the simulated burner annulus, and the operation of the compressor bearings.

An initial investigation at an equivalent compressor speed of 8000 rpm was made to determine the performance of the compressor and the collecting chamber and to determine the [illegible]larity of the air stream at the entrance to the simulated burner annulus. The mechanical performance of the compressor over a range of actual compressor speeds from 3300 to 8000 rpm is reported.

APPARATUS AND PROCEDURE

Compressor

The compressor assembly of the XJ-41-V turbojet engine consists of a single-entry centrifugal impeller, a vaneless diffuser followed by a vaned collector, and accessory shrouds and casings (fig. 1).

The impeller has an inlet tip diameter of 21.38 inches, a discharge tip diameter of 32.00 inches, 18 full blades, and 18 splitter blades. The flow path through the vaned collector has an increasing and then a decreasing radius of rotation and the essential function of the vaned collector is therefore to decrease the moment of momentum of the air. The radius of the outer entrance edge of the vanes is 20.40 inches, the maximum radius of the vaned collector is 23.75 inches, and the outer radius of the vaned collector at the discharge is 16.00 inches. The vaned collector is designed to have no radial component of flow at the discharge.

Compressor Installation

The compressor was mounted on a collecting chamber (fig. 2) having an annular passage that simulates the burner annulus of the engine. The collecting chamber was designed to maintain uniform flow in the annulus and care was taken to avoid the possible limitation of the compressor-flow capacity by choking in the chamber. The resulting collecting-chamber design causes a large loss in the dynamic pressure of the air at the collecting-chamber discharge. The compressor was driven by a 6000-horsepower electric motor with a speed-increaser gear for a maximum shaft speed of 12,000 rpm. The inlet pipe was 24 inches in diameter and 12 diameters long; the discharge pipe was 16 inches in diameter and 5 diameters long. No insulation material was used on the compressor, the collecting chamber, the inlet, and the discharge pipes. Two auxiliary oil systems lubricated the compressor bearings. A high-pressure pump supplied oil to the compressor bearings and a high-capacity pump scavenged the bearings.

Mechanical Operation of Compressor

Because the compressor thrust bearings were designed to carry only a partial impeller thrust load and depended upon the turbine thrust in the engine installation to balance a large part of the impeller thrust, six bearing thermocouples were installed to maintain a check on the mechanical performance of the compressor. An impeller-clearance warning instrument maintained a constant check on the safe-operating clearances between the impeller and the stationary shroud.

Before any aerodynamic data were taken, preliminary runs over a range of actual compressor speeds from 3300 to 8000 rpm were made. The compressor had stable and smooth mechanical operating characteristics over this range of speeds. Compressor-bearing temperatures noted over the speed range are shown in figure 3. A temperature of 300° F was set by the manufacturer as the maximum safe operating thrust bearing temperature. The effect of varying the oil-supply pressure to the thrust bearings was investigated at an actual compressor speed of 6000 rpm. Varying the oil-supply pressure from 50 to 20 pounds per square inch resulted in an approximate linear increase in bearing temperature, and a maximum increase in the front thrust bearing temperature of about 15° F was observed. Operating temperatures for the compressor bearings at an equivalent compressor speed of 8000 rpm over the volume-flow range are shown in figure 4.

Instrumentation

The compressor was extensively instrumented to determine the over-all performance of the compressor, the characteristic performance of each of the compressor components, and the state of the air stream in the simulated burner annulus. Instrumentation for determining over-all compressor performance, as recommended in references 1 and 2, was adopted wherever applicable. Along the flow path through the compressor, 104 static-pressure measurement taps were installed to determine the performance of the impeller and diffuser. Two pressure probes of the Fechheimer type (reference 3) were provided to measure the angularity of the air stream and the total-pressure gradient across the flow passage at the entrance to the collector vanes and at the trailing edges. A pressure probe for measuring yaw was installed to determine the angularity of the air stream immediately behind the vaned collector where the air enters the simulated burner annulus. This probe was calibrated in a steady air stream having uniform static pressures across the flow passage. The accuracy of the angular measurements determined by this instrument is dependent upon the local static-pressure gradients present in the air-flow passage. The simulated burner annulus was equipped with 10 total-pressure, 13 static-pressure, and 15 temperature measuring stations for determining the air-stream conditions.

Air-flow and pressure regulation was provided by butterfly throttle valves in the inlet and the discharge pipes. An adjustable submerged orifice measured the quantity of air flow.

Test Procedure

The compressor was run at an equivalent rotative speed $N/\sqrt{\theta}$ of 8000 rpm (N, actual impeller rotative speed; θ, ratio of inlet stagnation temperature to standard-air temperature). All runs were made with ambient inlet-air temperature and an absolute inlet stagnation pressure of approximately 14 inches of mercury except in the flow cut-off range, where higher inlet pressures were used. Inlet pressures of 14 inches of mercury absolute were used in order that the complete range of compressor speeds might be investigated at the same inlet-pressure conditions.

The over-all performance of the compressor and collecting chamber was determined by pressure and temperature measurements in the inlet and the discharge pipes. Angle surveys of the air stream were made at radial increments of one-half inch across the flow passage at the entrance to the simulated burner annulus, and static pressures on the inner and outer walls of the annulus were measured at the same location.

RESULTS AND DISCUSSION

The over-all adiabatic efficiency (measured between inlet and discharge pipes) η_{ad}, the corrected volume flow $Q_{t,1}/\sqrt{\theta}$, and the corrected weight flow $W\sqrt{\theta}/\delta$ are shown in figure 5. The quantity $Q_{t,1}$ is the volume flow at stagnation condition at the impeller inlet; the quantity W is the measured mass flow; and δ is the ratio of inlet total pressure to standard air pressure. A peak adiabatic efficiency of 0.77 was obtained at a corrected volume flow of 29,010 cubic feet per minute. A maximum corrected mass flow of 47.89 pounds per second was obtained. Figure 6 shows over-all total-pressure ratio P_2/P_1 and corrected volume flow $Q_{t,1}/\sqrt{\theta}$. The highest pressure ratio was 2.14. The compressor had a volume-flow range, expressed as the ratio of maximum to minimum volume flow, of 2.4. During the performance runs there was no evidence of mild or intermediate surging between maximum volume flow and surge.

The variation of the static pressures with volume flow at the entrance to the simulated burner annulus as measured at the inner and the outer walls of the flow passage is shown in figure 7. The general shape of the pressure-ratio curves and the magnitude of the pressure ratios indicate that the collecting chamber did not limit the compressor flow capacity and that the static pressures at the compressor discharge were approximately equal to the total pressures at the collecting-chamber discharge on which over-all performance is based. The outer-wall static pressures were considerably higher than the inner-wall static pressures over the volume-flow range.

The results of the angular surveys across the flow passage are shown in figure 8 for four runs at the entrance to the simulated burner annulus. The tangential angle is the angle between the impeller axis and the vector representing the resultant velocity of the axial and the circumferential components. The radial angle is the angle between the impeller axis and the vector representing the resultant velocity of the axial and the radial components. Inasmuch as these angles are dependent upon the static pressure at each measuring station, a knowledge of the static-pressure distribution across the passage is necessary. For convenience in this preliminary investigation, the flow angles as presented in figure 8 are based on an arithmetical average of the two wall static pressures. The variations in the measured flow angles that may result from the static-pressure gradient are shown in figure 9 for peak adiabatic efficiency. These angles were determined from the instrument calibration using the arithmetical average of the two wall static pressures and using the outer- and inner-wall static pressures independently. The actual angular gradient across the passage is probably less than that shown by any of the curves in figures 8 and 9. At maximum adiabatic efficiency, the tangential angle in the flow passage at the entrance to the simulated burner annulus was of the order of 75°, and the radial angle was of the order of 3°. The tangential-angle variation was small with volume flow. The radial-angle variation was small with volume flow except at surge where the radial angles increased appreciably. A recheck of the installation of the survey instrument after completion of the performance runs showed a misalinement in the survey tube of about 5°, which would make the tangential angles presented in figures 8 and 9 approximately 5° too low.

SUMMARY OF RESULTS

From an investigation of the performance characteristics of the XJ-41-V turbojet-engine compressor mounted on a collecting chamber, the following results were obtained:

1. The compressor had stable and smooth mechanical operating characteristics over a range of actual compressor speeds from 3300 to 8000 rpm.

2. At an equivalent compressor speed of 8000 rpm, the maximum over-all adiabatic efficiency between inlet and discharge pipes was 0.77 and the maximum pressure ratio was 2.14.

3. The maximum corrected mass flow was 47.89 pounds per second.

4. A static-pressure gradient existed across the flow passage at the entrance to the simulated burner annulus.

5. At maximum adiabatic efficiency, the tangential angle in the flow passage at the entrance to the simulated burner annulus was of the order of 75°, and the radial angle was of the order of 3°. The tangential-angle variation was small with volume flow. The radial-angle variation was small with volume flow except at surge where the radial angles increased appreciably.

Aircraft Engine Research Laboratory,
National Advisory Committee for Aeronautics,
Cleveland, Ohio.

Ambrose Ginsburg,
Mechanical Engineer.

John W. R. Creagh,
Electrical Engineer.

Approved:

Robert O. Bullock,
Mechanical Engineer.

Oscar W. Schey,
Mechanical Engineer.

vab

REFERENCES

1. Ellerbrock, Herman H., Jr., and Goldstein, Arthur W.: Principles and Methods of Rating and Testing Centrifugal Superchargers. NACA ARR, Feb. 1942.

2. NACA Subcommittee on Supercharger Compressors: Standard Procedures for Rating and Testing Centrifugal Compressors. NACA ARR No. E5F13, 1945.

3. Fechheimer, Carl J.: Measurement of Static Pressure. Mech. Eng., vol. 49, no. 8, Aug. 1927, pp. 871-873; discussion, pp. 873-874.

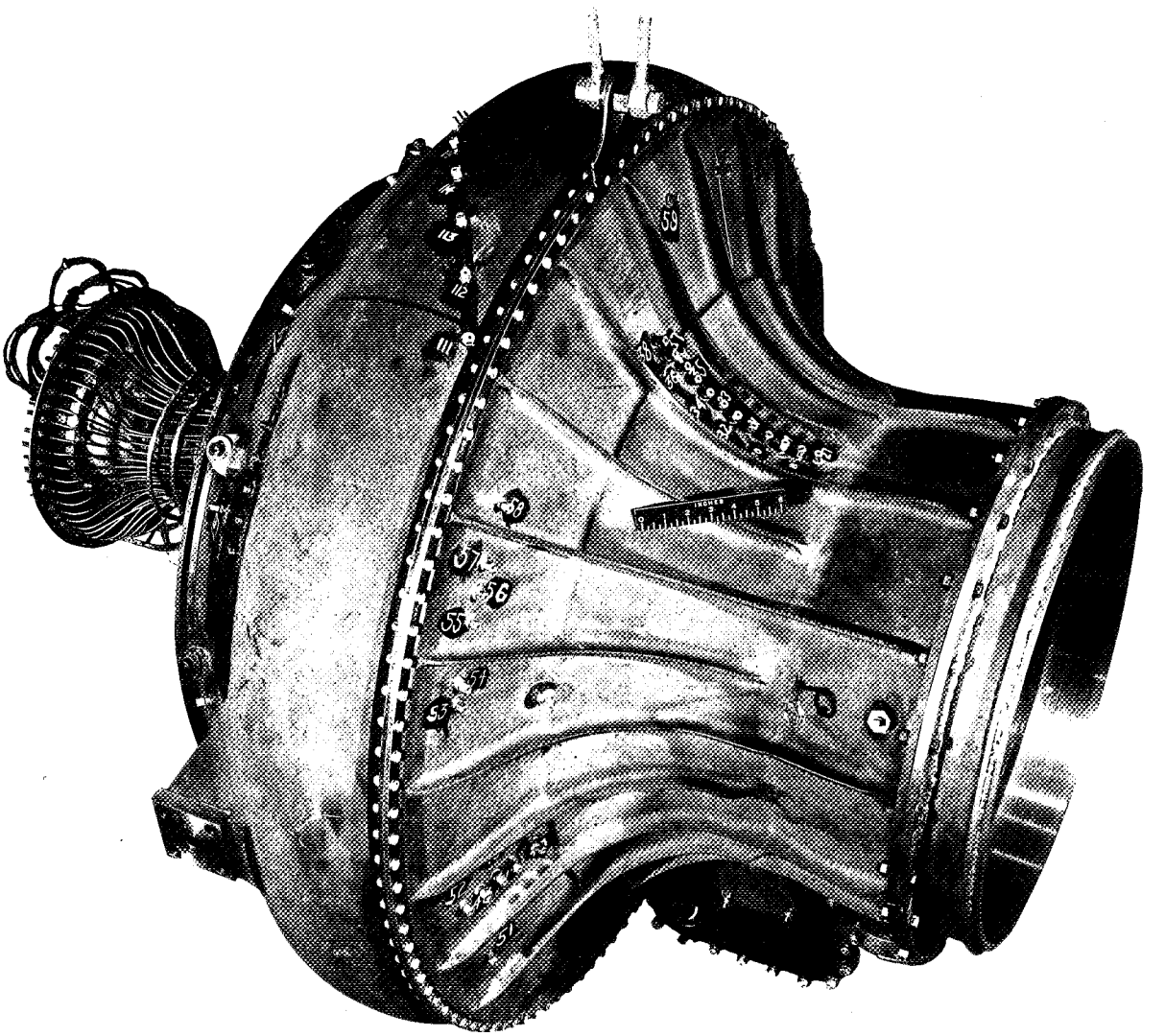

NACA
C-17001
10-21-46

Figure 1. - Compressor assembly of XJ-41-V turbojet engine.

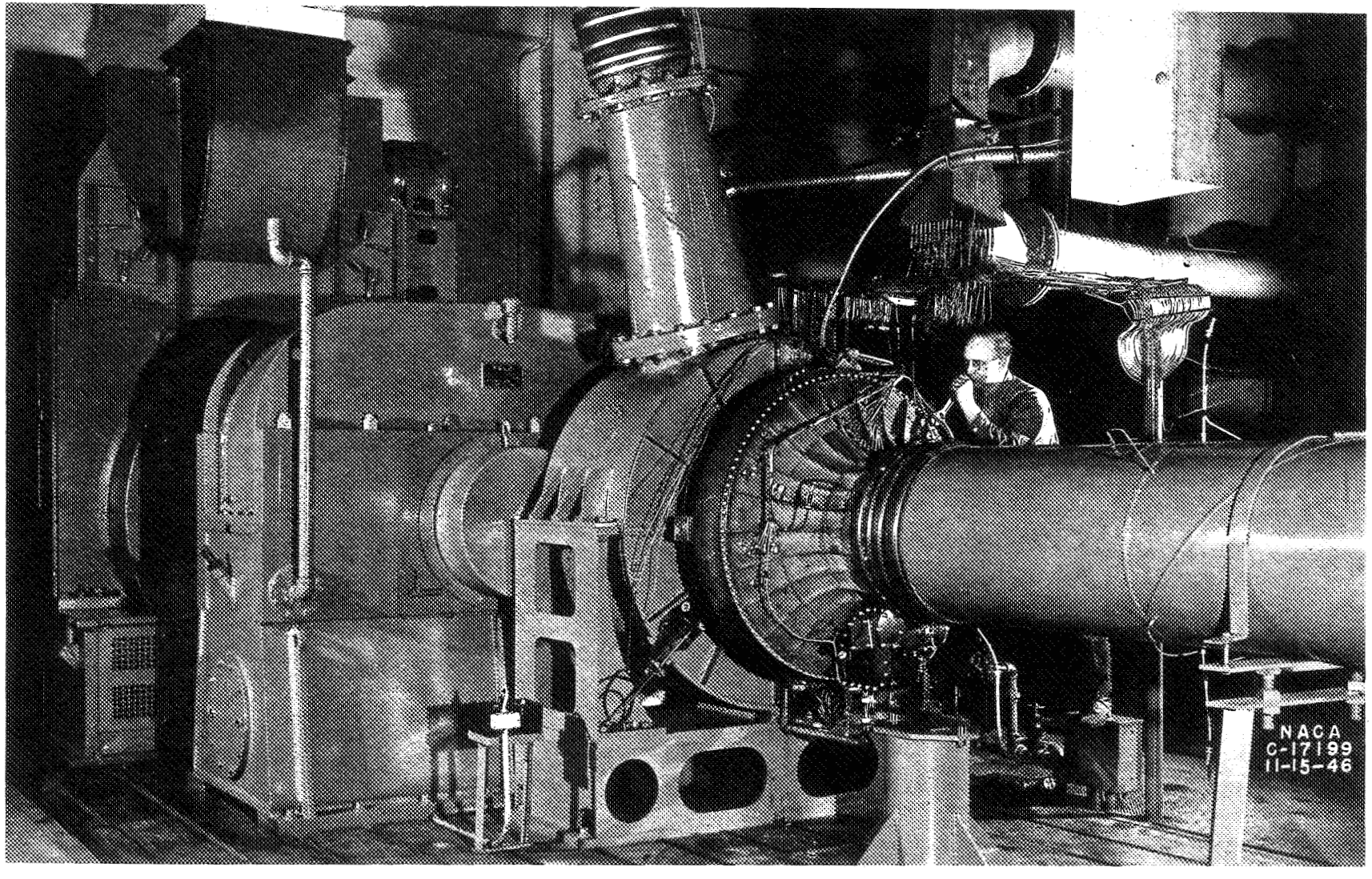

Figure 2. - Installation for performance investigation of compressor of XJ-41-V turbo-jet engine.

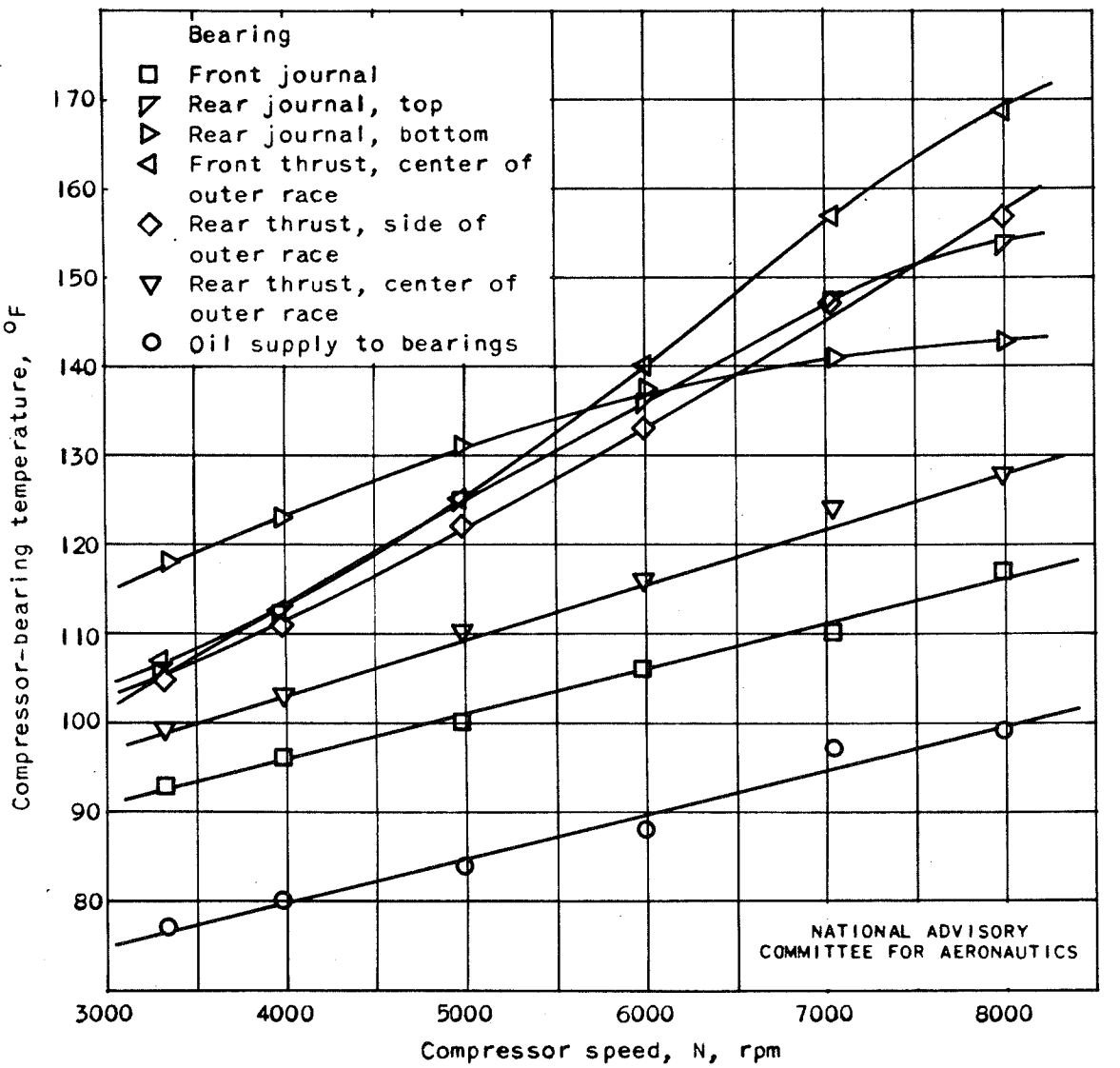

Figure 3. – Variation of compressor-bearing temperatures with compressor speed.

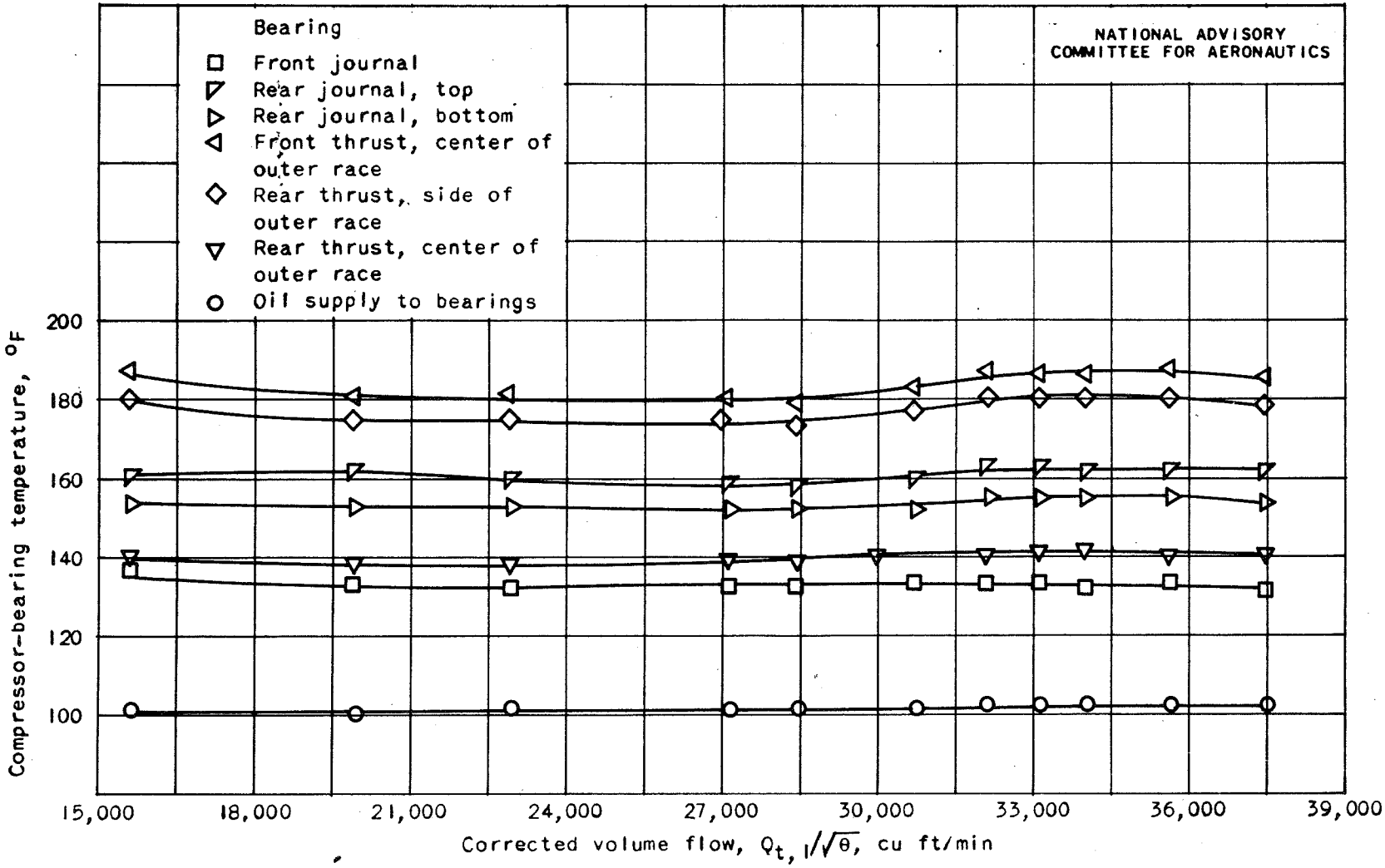

Figure 4. - Compressor-bearing temperatures at equivalent compressor speed of 8000 rpm.

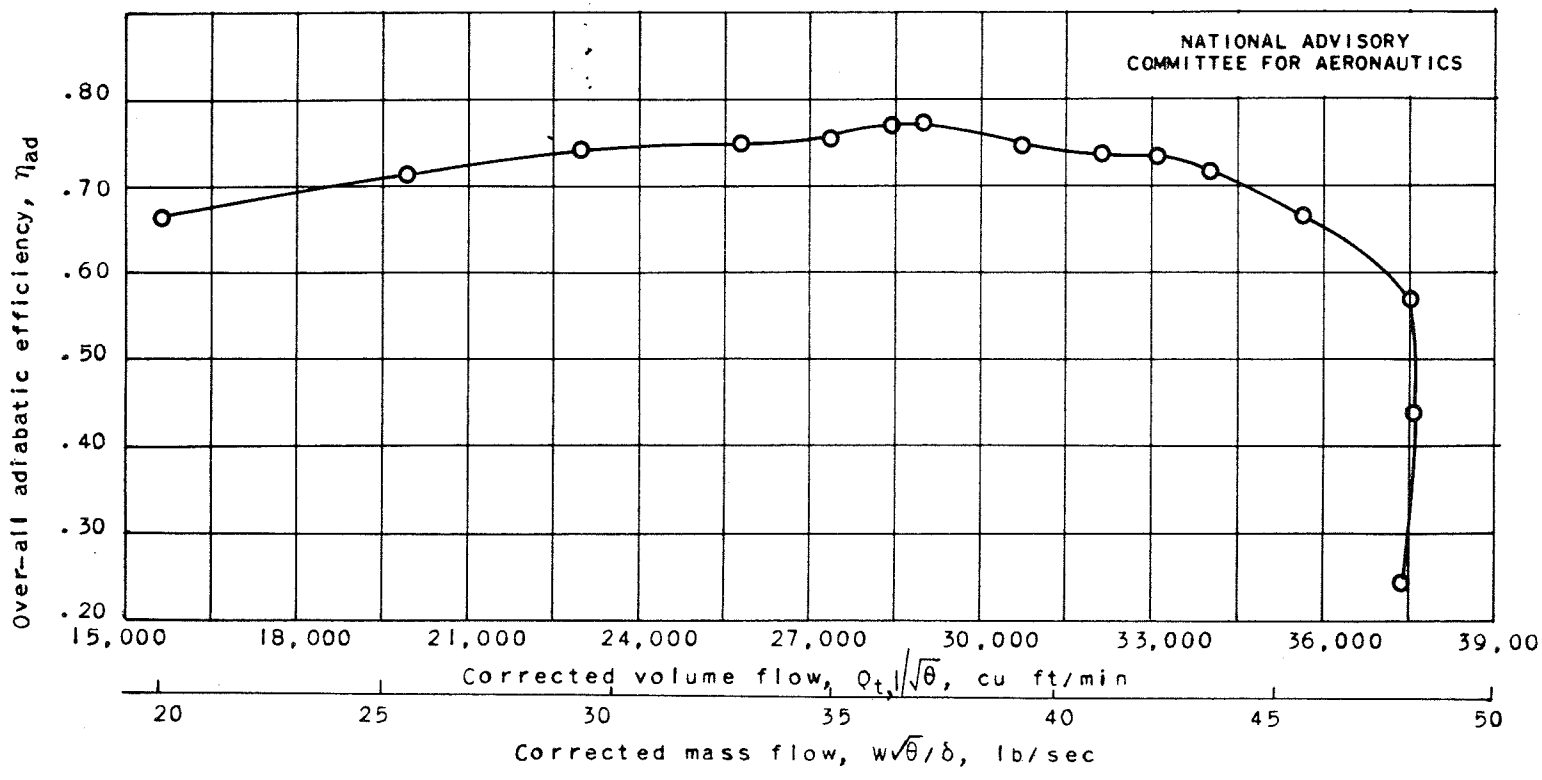

Figure 5. - Compressor and collecting-chamber over-all adiabatic efficiency at an equivalent compressor speed of 8000 rpm.

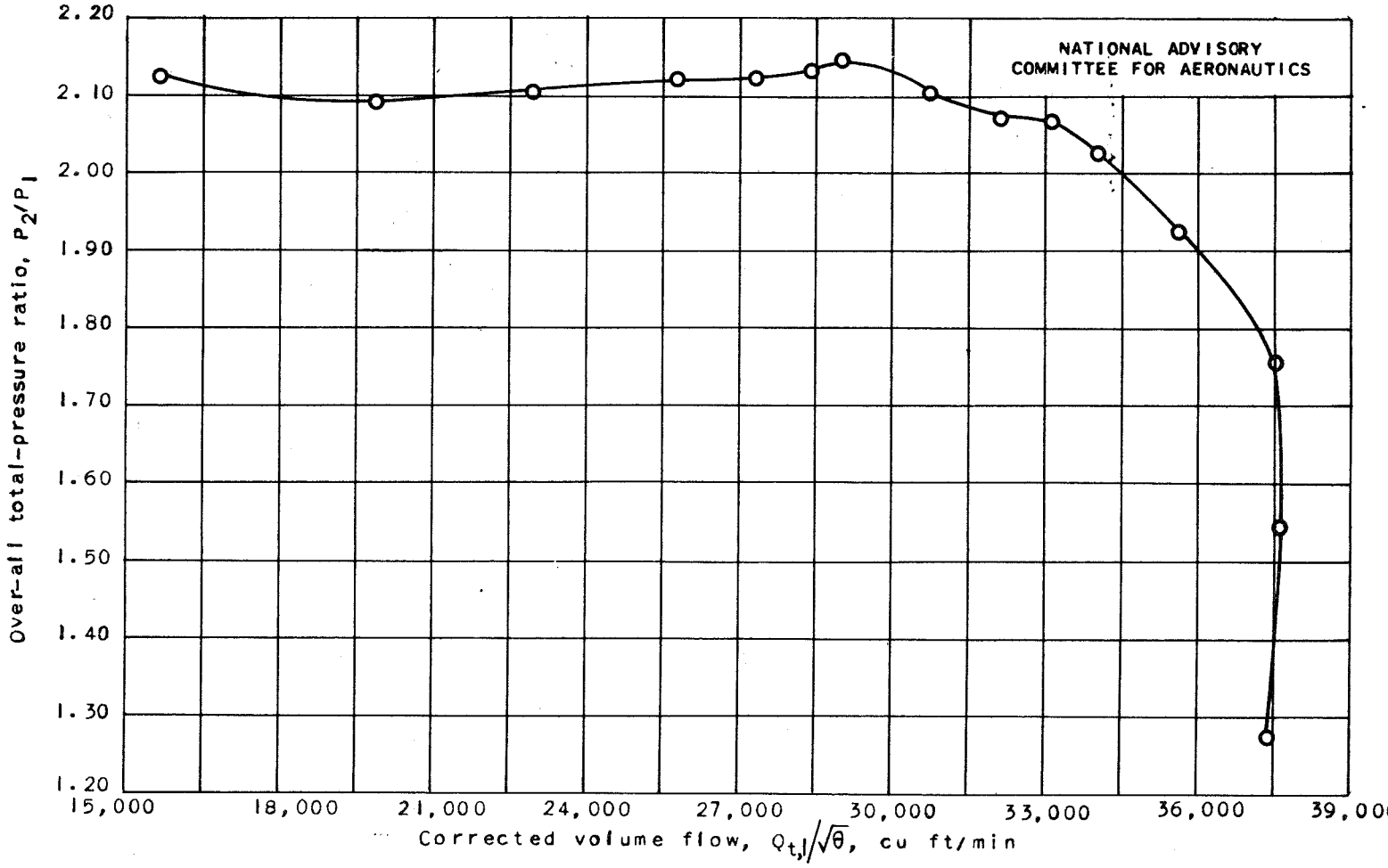

Figure 6. - Compressor and collecting-chamber total-pressure ratio at equivalent compressor speed of 8000 rpm.

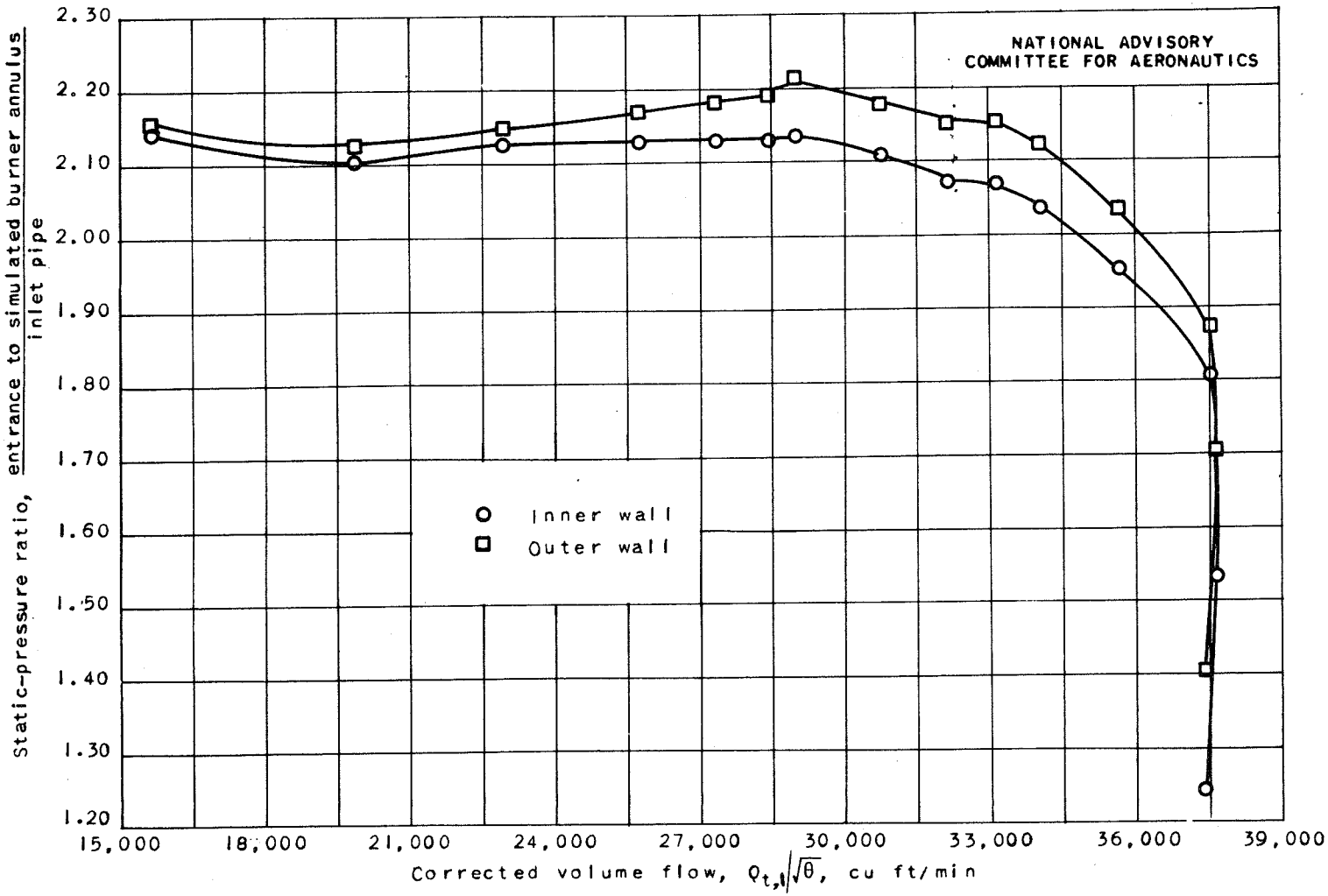

Figure 7. - Comparison of static pressures at entrance to simulated burner annulus as measured along inner and outer walls of flow passage at equivalent compressor speed of 8000 rpm.

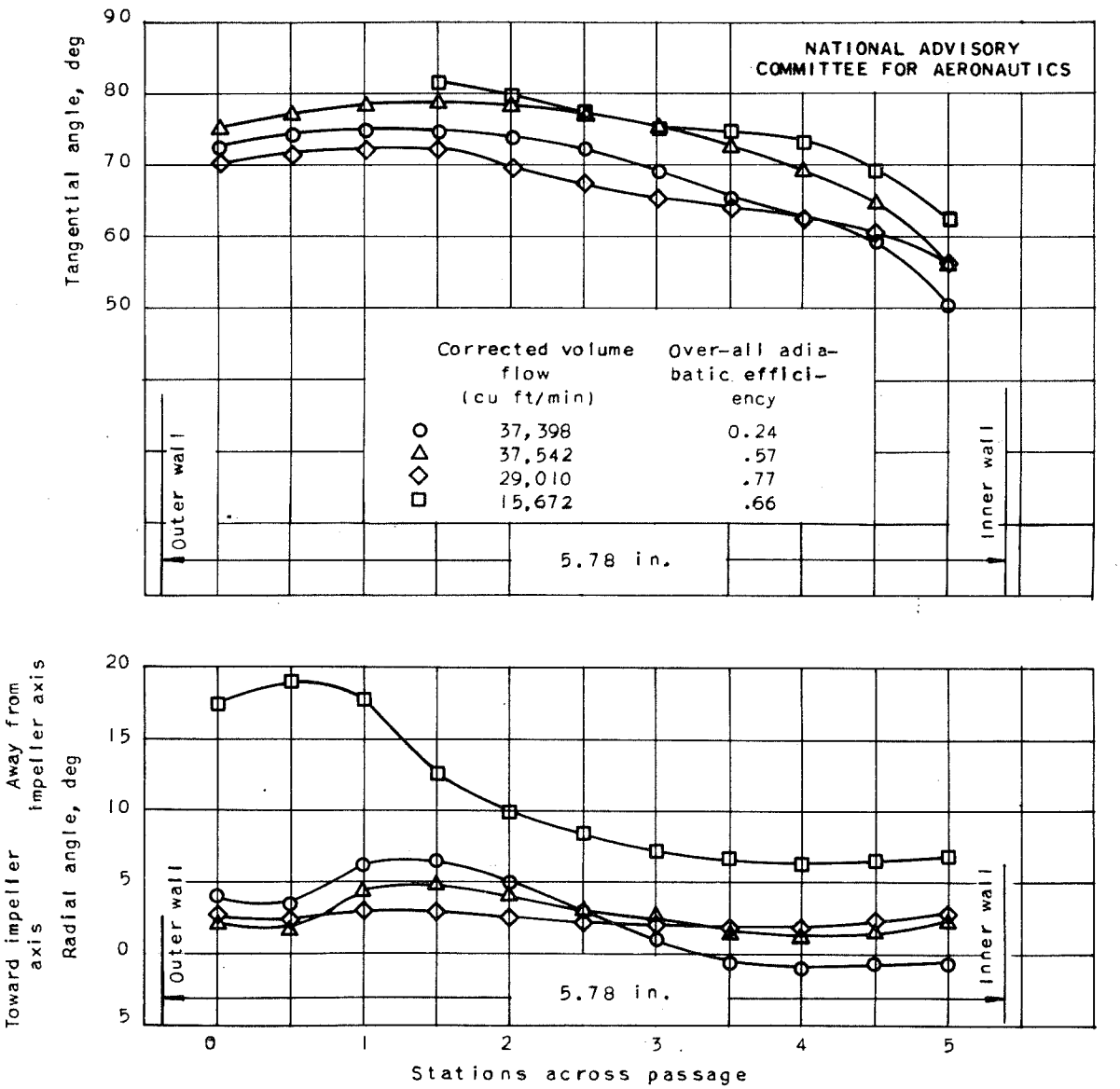

Figure 8. - Angular surveys of air stream across flow passage at entrance to simulated burner annulus at equivalent compressor speed of 8000 rpm.

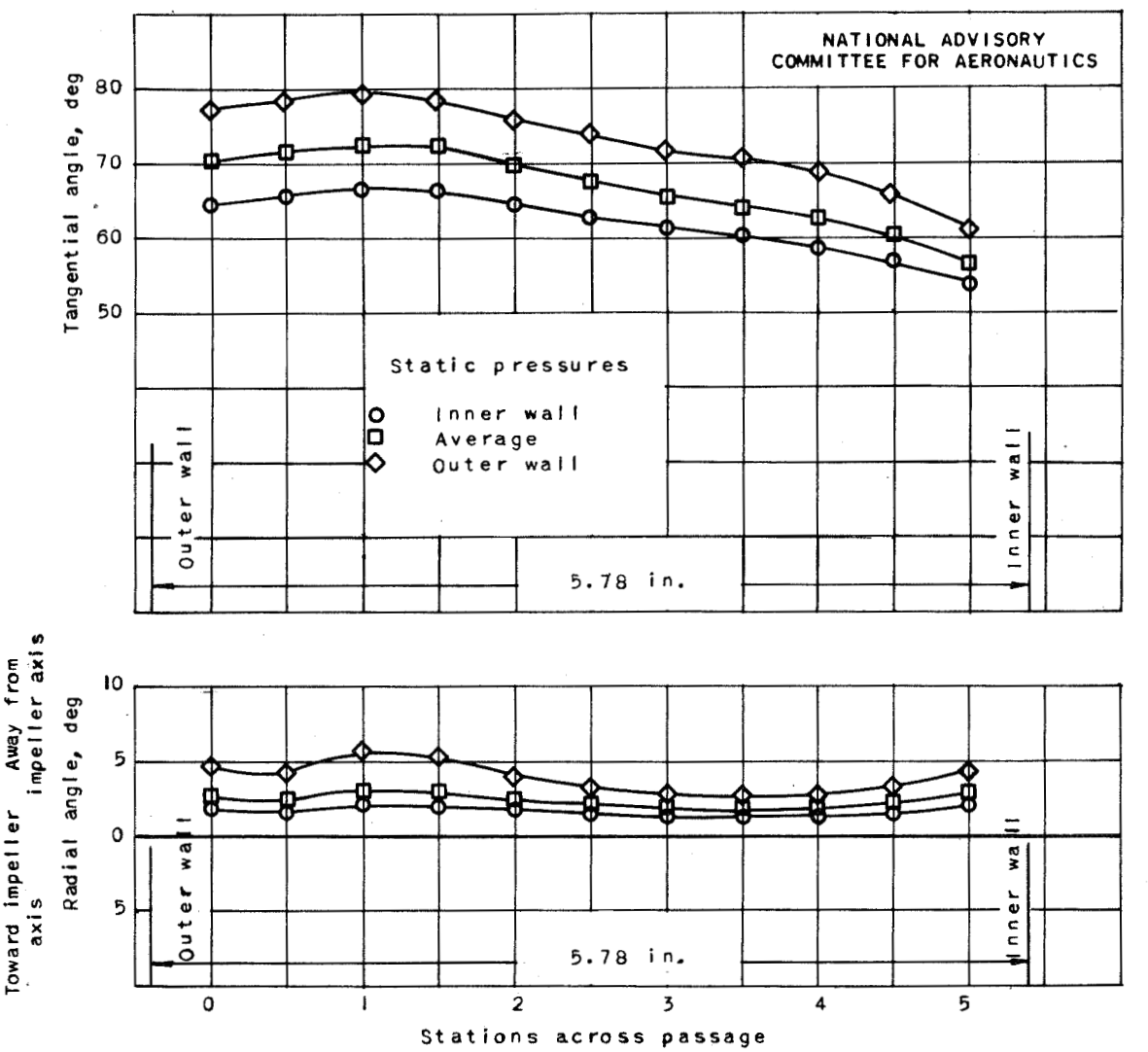

Figure 9. - Effects of static-pressure gradient across flow passage at entrance to simulated burner annulus on measured flow angles at peak adiabatic efficiency for equivalent compressor speed of 8000 rpm.